Electrochemical Characterization of Copper Paratolylsulfonate*

Song Ji-Guo Shen Pei-Kang

(State Key Laboratory of Optoelectronic Materials and Technologies, School of Physics Science and Engineering, Sun Yat-Sen University, Guangzhou 510275)

Abstract Copper(II) paratolylsulfonate [Cu(*p*-OTs)]$_2$ has been synthesized and characterized by X-ray crystal structure analysis. The electrochemical parameters of Cu(*p*-OTs)$_2$ in H_2O, CH_3OH and DMF have been studied on platinum electrode, respectively. Different reaction mechanisms in different solvents are found. The electrochemical reduction of Cu(II) to Cu proceeds by two one-electron steps in H_2O. However, it is a one two-electron process in CH_3OH and DMF.

Keywords: Copper paratolylsulfonate, Electrochemistry, Cyclic voltammetry, Mimetic enzyme

Copper complexes are involved in variety of important biochemical processes. Some copper complexes with different types of ligands have been synthesized and studied as mimetic enzyme[1-2]. Electrochemical techniques were used to characterize their electrochemical behaviors since the biochemical reactions related to the redox processes[3-4].

In the present paper we report the preparation of copper paratolylsulfonate(Cu(*p*-OTs)$_2$) and the results characterized by different methods. It has been found that Cu(*p*-OTs)$_2$ can lose all the crystal water easily and the dehydrated salt does not deliquesce in the air. Preliminary study shows that the complex of Cu(*p*-OTs)$_2$/ethanolamine(molar ratio is 1 : 1) can be used as mimetic enzyme. The electrochemical behaviors of Cu(*p*-OTs)$_2$ solution in H_2O, CH_3OH and DMF are described.

1 Experimental

1.1 Apparatus

The electrochemical measurements were carried out on a French VoltaLab 80 electrochemical workstation(Radiometer Analytical). The working electrode was a Pt (99.9%) wire (ϕ = 0.1 cm, area is 0.073 cm^2) and the counter electrode was a Pt (99.9%) sheet(1.0 cm × 1.0 cm). The saturated calomel electrode(SCE) was used as reference electrode. All the potential values in this paper were versus SCE. Purified argon was bubbled through the electrolytic solution to remove oxygen. The electrochemical measurements were carried out in an argon atmosphere at room temperature(25 ± 1) ℃.

1.2 Reagents

N, *N*-dimethylformamide(DMF) and CH_3OH were distilled under vacuum after adding 0.4 nm molecular sieves to remove water. The supporting electrolyte tetrabutyl ammonium perchlorate((n-Bu)$_4NClO_4$ or TBAP) was prepared following the literature[5]. Copper paratolylsulfonate was prepared by the reaction of CuO(99.95%) and p-$CH_3C_6H_4SO_3H \cdot H_2O$. The freshly prepared salt was dehydrated at 120 ℃ under 0.5 ~ 1.0 kPa and preserved in a desiccator containing anhydrous $CaCl_2$ for using in the electrochemical experiments. Unless stated otherwise, all the reagents were analytical pure. Aqueous solutions were prepared by double distilled water.

2 Results and Discussion

2.1 Analysis of copper paratolylsulfonate

The freshly prepared copper paratolylsulfonate is blue and has the molecular formula of Cu(p-$CH_3C_6H_4SO_3$)$_2 \cdot 6H_2O$. It was proved by X-ray crystal structure analysis as shown in Fig. 1. The DSC and TG experiments showed that this salt could lose all crystal water easily and the dehydrated salt does not deliquesce in the air[6]. Cu(*p*-OTs)$_2$ has been shown to have octahedral coordination of copper ions with a [CuO_6] skeleton in which OTs^- acts as tridentate bridging ligands through the three oxygen atoms bonded to sulfur[7]. OTs^- is a multi-dentate ligand, therefore, the Cu(*p*-OTs)$_2$ is suitable for the electrochemical studies in nonaqueous solvents.

2.2 The electrochemical behavior of Cu(*p*-OTs)$_2$ in H_2O

Received: March 10, 2004; Revised: May 28, 2004. Correspondent: Shen Pei-Kang(E-mail: stdp32@zsu.edu.cn; Tel&Fax: 86-20-84113369). *The Project Supported by the Grant 863 Program of China(2003AA517050) and the Guangzhou Science and Technology Project (2003Z2-D0081)

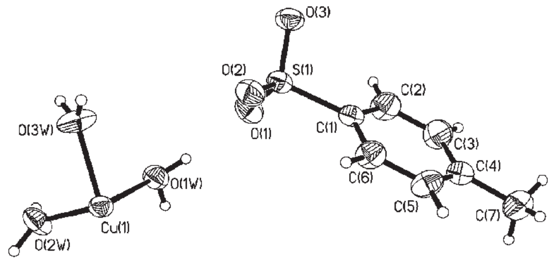

Fig. 1 The X-ray structure of Cu(*p*-OTs)$_2$·6H$_2$O

The cyclic voltammograms of Pt electrode in Cu(*p*-OTs)$_2$/KCl aqueous solution at different scan rates are shown in Fig. 2. There are two pairs of redox peaks as shown in the figure. The relationship between the first cathodic peak current (I_p) and the square root of the scan rate ($v^{1/2}$) is linear as shown in the inset of Fig. 2. The surface of Pt electrode kept clean after 5 min electrolysis at the potential of 0.1 V(at the first cathodic peak). However, red color appeared on the Pt electrode after 5 min electrolysis at the potential of −0.2 V(at the second cathodic peak). It is proved that the electrochemical reduction of Cu(*p*-OTs)$_2$ in aqueous solution is through two steps.

The potential of the first cathodic peak E_{pc} in Fig. 2 does not change with the potential sweep rate. The first cathodic peak current(I_{pc}) is equal to the corresponding anodic peak current(I_{pa}). The plot of the peak current I_p with the square root of sweep rate $v^{1/2}$ for the first cathodic peak is linear, as shown in the inset of Fig. 2. For a reversible electron transfer, $\Delta E_p = E_{pa} - E_{pc} = 2.3RT/nF$[5], where n is calculated to be 0.98 with the E_p values of Fig. 2, indicating that the electron transfer number is one. Therefore, the reduction of Cu(II) to Cu proceeds by two steps of one electron transfer. All the above characteristics indicate that the electro-reduction of Cu(II) to Cu(I) is reversible.

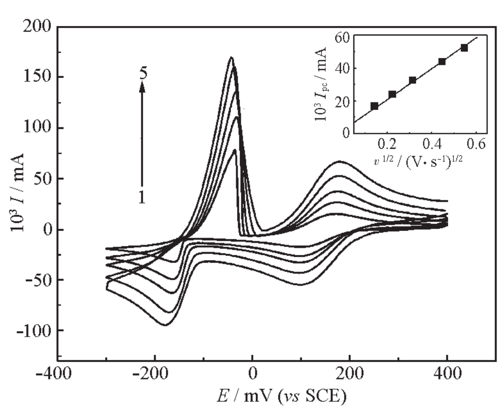

Fig. 2 Cyclic voltammograms of 0.012 mol·L^{-1} Cu(*p*-OTs)$_2$/0.1 mol·L^{-1} KCl aqueous solution

inset: linear relationship between peak current and the square root of scan rate. *T*: 298 K; scan rates (V·s^{-1}): 1)0.02; 2)0.03; 3)0.1; 4)0.2 and 5)0.3

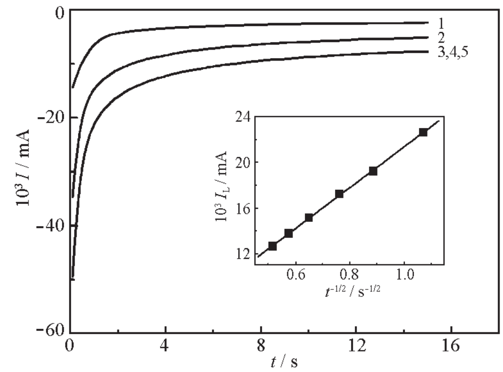

Fig. 3 Chronoamperograms of 0.012 mol·L^{-1} Cu(*p*-OTs)$_2$/0.1 mol·L^{-1} KCl in H$_2$O

constant potentials (V): 1)0.15; 2)0.12; 3)0.08; 4)0.05 and 5)0.03

inset: linear relationship between steady-state current (I_L) and $t^{-1/2}$.

For the soluble reactant and soluble product, the reversible charge transfer obeys the Randles-Sevĉik equation[8]

$$I_p = 0.4463(nF)^{3/2}(Dv / RT)^{1/2}Ac \quad (1)$$

Where I_p, n, D, v, A, T and c represent the peak current, electron number, diffusion coefficient, scan rate, area of work electrode, temperature and Cu^{2+} concentration, respectively. $R = 8.314$ J·mol·L^{-1}, $F = 96485$ C·mol^{-1}.

According to the slope of the line in the inset of Fig. 2 and equation(1), the diffusion coefficient of Cu(*p*-OTs)$_2$ in KCl aqueous solution at 298 K was calculated as 1.65×10^{-7} cm^2·s^{-1}.

Fig. 3 shows the chronoamperometric curves in Cu(*p*-OTs)$_2$/KCl aqueous solution at different potential steps. The curves at potentials less than 80 mV were overlapped because of the limiting current electrolysis for Cu(II) to Cu(I) process. The plot of $I_L - t^{-1/2}$ was linear (inset of Fig. 3), from that the diffusion coefficient can be calculated according to the cottroll equation[8]

$$I_L = nF\pi^{-1/2}AcD^{1/2}t^{-1/2} \quad (2)$$

Where I_L is limit diffusion current, $\pi = 3.14$.

From the equation (2) and the slope of the line in the inset of Fig. 3, the diffusion coefficient was calculated as 1.66×10^{-7} cm^2·s^{-1} which agrees with the diffusion coefficient calculated by cyclic voltammetry.

Fig. 4 is the chronopotentiometric curve in Cu(*p*-OTs)$_2$/KCl aqueous solution. The reductive current was controlled at −0.065 mA. The open circuit potential is 250 mV. Two plateaus at 150 mV and −130 mV appeared on the $E - t$ curve. These potentials are in accord with the starting potentials of the cathodic peaks in the Fig. 2. The two plateaus correspond to Cu(II)/Cu(I) and Cu(I)/Cu reactions respectively, indicating that the reduction of Cu(II) in aqueous solution proceeds

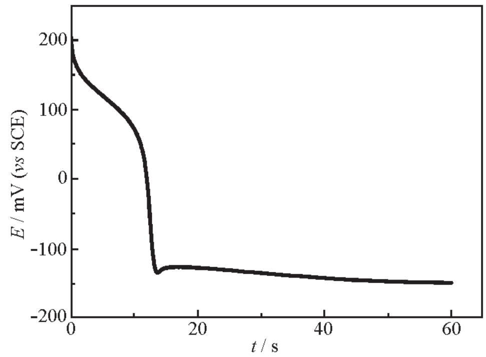

Fig. 4 The response of constant current polarization at −0.065 mA in 0.012 mol·L^{-1} Cu(*p*-OTs)$_2$/ 0.1 mol·L^{-1} KCl aqueous solution, 298 K

by two steps.

Sometimes it needs additional overpotential at the beginning of the formation of new phase, which is corresponding to the result that a maximum point appeared on the plateaus[9]. The second plateau is the electro-reduction from Cu(I) to Cu. A new phase (solid Cu) deposits on the Pt electrode in the process, so a maximum point appears at the beginning of the second plateau.

2.3 The electrochemical behavior of Cu(*p*-OTs)$_2$ in CH_3OH

Fig. 5 shows the cyclic voltammograms of Cu(*p*-OTs)$_2$/TBAP/CH_3OH system on a Pt electrode at different scan rates. There was only one pair of redox peaks on the curve. The surface of Pt electrode appeared yellow compact deposit after 5 min electrolysis at the potential of cathodic peak. Because of the known valence states of copper, it is considered that the cathodic peak is due to the reduction of Cu(II) to Cu and the anodic peak corresponds to the anodic stripping of Cu. The result indicates that the electrochemical reduction of Cu(*p*-OTs)$_2$ in CH_3OH is a one-step process.

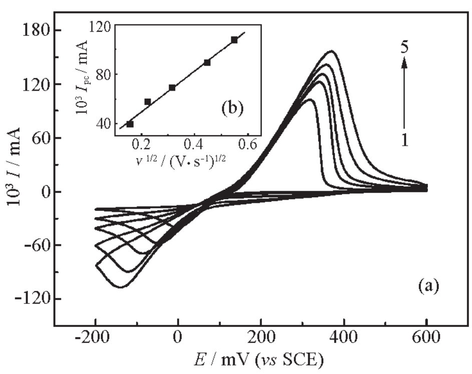

Fig. 5 (a)The CV curves of 0.05 mol·L^{-1} TBAP + 0.011 mol·L^{-1} Cu(*p*-OTs)$_2$ in CH_3OH and (b)$I_p - v^{1/2}$ curve

T: 298 K, scan rates (V·s^{-1}): 1)0.02; 2)0.05; 3)0.1; 4)0.2; 5)0.3

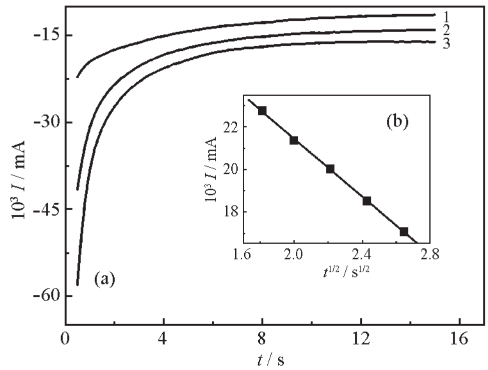

Fig. 6 (a)Chronoamperograms of 0.05 mol·L^{-1} TBAP + 0.011 mol·L^{-1} Cu(*p*-OTs)$_2$ in CH_3OH and (b)$I - t^{1/2}$ curve

constant potentials(V): 1)0.05; 2) −0.05; 3) −0.15

The potential of cathodic peak, E_{pc} in Fig. 5a, changed with the change of scan rate. The relationship between the cathodic peak current (I_p) and the square root of the scan rate($v^{1/2}$) is linear as shown in Fig. 5b. With the increase of the scan rate, the cathodic peak potential shifts negatively and the anodic peak potential shifts positively. For the reversible electron transfer, $\Delta E_p = E_{pa} - E_{pc} = 2.3RT/nF$[5]. The datum of $E_{pa} - E_{pc}$ equals to $(60/n)$ mV in lower scan rate for the quasi-reversible electron transfer[8]. The electron transfer number (n) is 2 in the electrochemical reduction of Cu(*p*-OTs)$_2$ in CH_3OH. The $E_{pa} - E_{pc}$ can be calculated as 310 mV at lower scan rate (20 mV·s^{-1}) in Fig. 5a which is 10 times larger than 30 mV. On the other hand, I_{pa} and I_{pc} are 0.109 mA and 0.033 mA respectively in 20 mV·s^{-1}, $I_{pa}/I_{pc} \neq 1$. All the above characteristics indicate that the electro-reduction of Cu(II) to Cu is irreversible.

For the irreversible electrode process[8]:

$$|E_p - E_{p/2}| = 1.857RT/(\alpha n_\alpha F) \quad (3)$$

Where E_p, $E_{p/2}$, α and n_α are the peak potential, half peak potential, transfer coefficient and electron number in the rate-determining step, respectively.

The α is calculated according to the data on the CV curve at 20 mV·s^{-1} and the value is 0.54.

The irreversible charge transfer obeys the Randles-Sevĕik equation[8]:

$$I_p = 0.4958\ n(F)^{3/2}\ (\alpha n_\alpha Dv\ /\ RT)^{1/2} Ac \quad (4)$$

According to the slope of the line in Fig. 5b and equation (4), the diffusion coefficient of Cu(II) in Cu(*p*-OTs)$_2$/TBAP/CH_3OH at 298 K was calculated as 1.44×10^{-7} cm^2·s^{-1}.

Fig. 6 is the chronoamperometric curves in TBAP/Cu(*p*-OTs)$_2$/CH_3OH solution at different potential steps. The Faraday current was found when the potential steps from rest potential to −0.15 V. The plot of $I - t^{1/2}$ is linear (Fig. 6b) which accords with the equation[8]:

$$I = nFAk_f c\ (1 - 2k_f\ t^{1/2}/\pi^{1/2} D^{1/2}) \quad (5)$$

Where k_f is reaction rate constant.

From the equation (5) and the slope of the line in Fig. 6b, diffusion coefficient D was calculated as 3.60×10^{-7} $cm^2 \cdot s^{-1}$ (error is 0.1%, reliability is 0.9997) which is larger than the value of D calculated from the cyclic voltammogram.

2.4 The electrochemical behavior of Cu(p-OTs)$_2$ in DMF

The cyclic voltammograms of Pt electrode in Cu(p-OTs)$_2$/TBAP/DMF are shown in Fig. 7. Only one pair of cathodic peak and anodic peak appeared. There was a black compact deposit after 5 min galvanostatic electrolysis at the cathodic peak potential, so the electroreduction of Cu(p-OTs)$_2$ in DMF is through one step. The potential of cathodic peak (E_{pc}) in Fig. 7a changed with the change of scan rate. The plot of peak current (I_p) against the square root of scan rate ($v^{1/2}$) is linear as shown in Fig. 7b. The $E_{pa} - E_{pc}$ can be calculated as 303 mV at 20 $mV \cdot s^{-1}$ in Fig. 7a which is 10 times larger than 30 mV. On the other hand, I_{pa} and I_{pc} are 0.055 mA and 0.034 mA respectively in 20 $mV \cdot s^{-1}$, $I_{pa} / I_{pc} \neq 1$. All the above characteristics indicate that the electro-reduction of Cu(II) to Cu is irreversible. The transfer coefficient α was calculated as 0.48 according to equation (3).

According to the slope of the line in the Fig. 7b and equation (4), the diffusion coefficient of Cu(II) in Cu(p-OTs)$_2$/TBAP/DMF at 298 K was calculated as 0.49×10^{-7} $cm^2 \cdot s^{-1}$. The viscosity of DMF is 7.96×10^{-3} poise and that of CH_3OH is 5.43×10^{-3}poise[10], so the diffusion coefficient in DMF is smaller than that in CH_3OH.

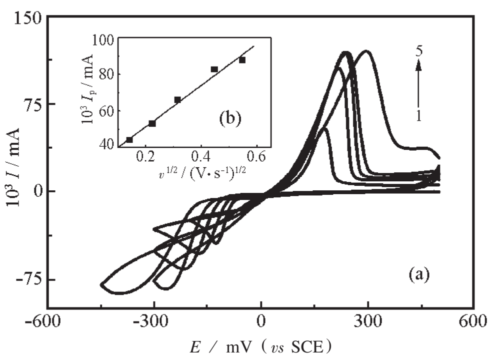

Fig. 7 (a) The CV curves of 0.05 mol·L^{-1} TBAP + 0.012 mol·L^{-1} Cu(p-OTs)$_2$ in DMF and (b) $I_p - v^{1/2}$ curve

temperature: 298 K, scan rate ($V \cdot s^{-1}$): 1) 0.02; 2) 0.05; 3) 0.1; 4) 0.2; 5) 0.3

3 Conclusions

The electrochemical parameters of Cu(p-OTs)$_2$ have been studied on platinum electrode in H_2O, CH_3OH and DMF media. The electrochemical reduction of Cu(II) to Cu proceeds by two one-electron steps in H_2O. However, it is through one step in CH_3OH and DMF.

The solvation power of both CH_3OH and Cu(p-OTs)$_2$ is weak, Cu(II) and OTs^- exist as tight ion pair with high static power, so that the reductive energy of Cu(p-OTs)$_2$ in CH_3OH is high and the diffusion coefficient is small.

The solvation power of DMF is stronger than that of CH_3OH, the reductive energy in DMF is larger than that in CH_3OH, so the cathodic peak potential in DMF is more negative than that in CH_3OH. On the other hand, Cu(II) can be solvated by DMF better than that by CH_3OH. Therefore the oxidation of Cu becomes easier in DMF than in CH_3OH, resulting a more negative anodic peak potential in DMF compared with that in CH_3OH.

References

1 Wang, Y. D.; DuBois, J. L.; Hedman, B.; Hodgson, K. O.; Stack, T. D. P. *Science*, **1998, 279:** 537

2 Collman, J. P.; Fu, L.; Herrmann, P. C.; Zhang, X. M. *Science*, **1997, 275:** 949

3 Cabral, M. F.; Cabral, J. de O.; Bouwman, E.; Driessen, W. L.; Reedijk, J.; Turpeinen, U.; Hämälainen, R. *Inorg. Chem. Acta*, **1992, 196:** 137

4 Wieghardt, K.; Bossek, U.; Ventur, D.; Weiss, J. *J. Chem. Soc. Chem. Commun.*, **1985:** 347

5 Song, J. G.; Song, H. C.; Yang, Q. Q. *Rare Metals*, **2003, 22**(3): 210

6 Song, J. G.; Shen, P. K. *Electrochemistry*, *in press* [宋继国, 沈培康. 电化学(*Dianhuaxue*), 印刷中]

7 Kapila, V. P.; Kapila, B.; Kumar, S. *Indian J. Chem.*, **1991, 30A:** 908

8 Bard, A. J.; Faulkner, L. R. Electrochemical methods. New York: Wiley Press, 1980: 268

9 Tian, Z. W. Electrochemical research methods. Beijing: Science Press, 1984: 194 [田昭武. 电化学研究方法. 北京: 科学出版社, 1984: 194]

10 Donald, T. S.; Julian, R. J. Experimental electrochemistry for chemists. New York: John Wiley & Sons Press, 1979: 207

对甲苯磺酸铜的电化学表征*

宋继国　　沈培康

(中山大学物理科学与工程技术学院, 光电材料与技术国家重点实验室, 广州　510275)

摘要　合成了对甲苯磺酸铜, 用 X 光单晶衍射确定了其结构 . 实验结果表明, 该盐容易脱除全部结晶水, 在空气中不潮解 . 分别测定了对甲苯磺酸铜(Cu(*p*-OTs)$_2$)在 H_2O、CH_3OH 和 DMF 中的电化学参数 . 实验结果表明 Cu(*p*-OTs)$_2$ 在不同溶剂中的反应机理各异 . Cu(II) 的电化学还原在 H_2O 中是分两步进行, 而在 CH_3OH 和 DMF 中的电化学还原是一步两电子过程 . 对实验结果进行了分析讨论 .

关键词: 对甲苯磺酸铜, 电化学, 循环伏安法, 模拟酶

中图分类号: O646

2004-03-10 收到初稿, 2004-05-28 收到修改稿 . 联系人: 沈培康(E-mail: stdp32@zsu. edu. cn; Tel&Fax: 86-20-84113369). *国家高技术研究发展规划(863 项目 2003AA517050)和广州科技基金(2003Z2-D0081)资助项目